WILEY | Hindawi

Research Article

Tea Polysaccharide (TPS) Reduces Astrocytes Apoptosis Induced by Oxygen-Glucose Deprivation/Reoxygenation by Regulating the miR-375/SRXN1 Axis

Ying Jiang,[1] Hongmei Sun,[2] Zhiqi Yin,[3] and Jun Yan [ID][3]

[1]*Department of Clinical Laboratory, Tianjin First Center Hospital, Tianjin 300192, China*
[2]*Department of Out-patient, Tianjin First Center Hospital, Tianjin 300192, China*
[3]*Department of Pathology, Tianjin First Center Hospital, Tianjin 300192, China*

Correspondence should be addressed to Jun Yan; yanhuang2@163.com

Objective. To investigate the effect of tea polysaccharides (TPS) mediated by miR-375/SRXN1 axis on mice with cerebral ischemia-reperfusion injury and proliferation and apoptosis of astrocytes (AS) conducted with oxygen-glucose deprivation/reoxygenation (OGD/R). *Methods*. Mouse model of middle cerebral artery occlusion (MCAO) and OGD/R-induced AS injury model were established; brain obstruction volume was measured by TTC staining; dry/wet weight ratio was used for measuring brain water content; hydrogen peroxide (H_2O_2) content in brain tissue was measured by H_2O_2 assay kit; cell viability and apoptosis rate were detected by MTT assay and flow cytometry, respectively; the expression level of miR-375 in OGD/R-AS was detected using qPCR; dual-luciferase reporter assay was used to verify the targeting relationship between miR-375 and SRXN1; mRNA levels of miR-375, SRXN1, Bcl-2, Bax, and caspase-3 were measured by qPCR; the protein levels of SRXN1, Bcl-2, Bax, and caspase-3 were measured by Western blotting. *Results*. The volume of cerebral obstruction, brain water content and H_2O_2 content in mice decreased gradually with the increase of TPS concentration. TPS treatment in vitro could effectively improve OGD/R-AS viability and reduce the apoptotic rate; overexpression of miR-375 inhibited AS viability but increased the apoptotic rate; TPS treatment resulted in a decrease in the expression of miR-375 in OGD/R-AS; MiR-375 targeted SRXN1 in AS; inhibition of miR-375 expression significantly upregulated SRXN1 levels; TPS treatment with simultaneous overexpression of SRXN1 significantly increased OGD/R-AS activity and reduced apoptosis; however, TPS treatment with simultaneous overexpression of SRXN1 and miR-375 resulted in no significant difference in cell viability and apoptosis rate compared with the control group. *Conclusion*. TPS reduces astrocyte injury induced by cerebral ischemia-reperfusion in mice by regulating the miR-375/SRXN1 molecular axis.

1. Introduction

Ischemic stroke, one of the leading causes of interruption of cerebral blood flow, is also an important factor of death and disability worldwide [1]. Restoration of blood supply to the brain following ischemic stroke may lead to reperfusion injury [2]. Reperfusion stimulates the overproduction of reactive oxygen species (ROS) such as hydrogen peroxide (H2O2), which induces cell proliferation, growth arrest, and causes apoptosis and necrosis [3]. Astrocytes (AS), one of the major types of glial cells in the central nervous

system (CNS), have various functions of regulating blood-brain barrier permeability, glial scar formation, and synaptic activity [4]. There is increasing evidence that apoptosis and death of nerve cells after ischemia-reperfusion are the main causes of exacerbated brain injury [5]. Therefore, it is very urgent to develop novel therapeutic strategies for cerebral ischemia-reperfusion. Sulfiredoxin-1 (SRXN1) is an endogenous antioxidant protein [6] that plays an important role in neuroprotection [7]. SRXN1 can resist cellular oxidative stress-induced ROS production [8, 9]. Zhou et al. [10] reported the antioxidant function exerted by

SRXN1 in protecting rat cortical AS from apoptosis, confirming that SRXN1 is a potential target gene for the treatment of cerebral ischemia-reperfusion injury.

Tea polysaccharides (TPS) is heteropolysaccharides extracted from leaves, flowers, and seed peels of tea trees [11] and is mainly composed of arabinose, xylose, glucose, galactose, galactoglucan, pectin, and protein. In the past few decades, significant progress has been made in the study of the chemical and biological activities of TPS and other related tea products. TPS has many health benefits. It has antioxidant, antiaging, and antitumor effects, as well as the ability to reduce cerebral ischemia-reperfusion injury after stroke [12], to improve diabetes [13], to boost body immunity [14], and to reduce hepatotoxicity [15]. However, the molecular mechanism of its role in most diseases is unknown.

MicroRNAs (miRNAs) refer to a newly discovered class of endogenous noncoding RNAs, which are involved in posttranscriptional gene regulation by binding to target sites in the 3′-UTR of target mRNA and result in mRNA degradation or translation inhibition [16]. In an animal study, investigators analyzed miRNA profiles after cerebral ischemia-reperfusion and have found that high miR-375 expression was detected at 12 h of ischemia-reperfusion, while expressions of other up-regulated genes gradually peaked after 72 h. Therefore, miR-375 is expected to be a diagnostic and therapeutic target for cerebral ischemia-reperfusion [17]. It has been reported that miRNAs are stimulated by external factors to change their expressions, thereby specifically regulating the expressions of target genes. There have been some reports that polysaccharides exert anti-inflammatory and antioxidant effects in vitro by regulating the expression of miRNAs [18, 19]. However, there is no report that focused on the role of polysaccharides in regulating AS activity and alleviating cerebral ischemia-reperfusion injury via miRNA.

Therefore, in this study, we investigated the protective effect of TPS on AS after ischemia-reperfusion injury by establishing a MACO mouse model and an OGD/R and AS injury model and attempted to provide new insights on the role of TPS in reducing the oxidative stress-caused apoptosis. Our results showed that TPS could alleviate the brain damage caused by cerebral ischemia-reperfusion and reduce astrocyte apoptosis by regulating the miR-375/SRXN1 axis, which provided a new potential theoretical basis for the effect of polysaccharides on treating cerebral ischemia-reperfusion injury.

2. Materials and Methods

2.1. Materials

2.1.1. Animal Origin. Fifty-four male ICR mice, weighing 25-30 g, were purchased from Kay Biological Technology (Shanghai) Co., Ltd. Mice were housed in a 12 h light/12 h dark cycle in a constant temperature room, with daily feed and water provided regularly.

2.1.2. Cell Origin and Culture. Astrocytes (AS) were purchased from Shanghai Yu Bo Biological Technology Co., Ltd. (article number: HUM-YB-n012). The AS were adherently cultured in complete medium (DMEM/FBS) containing 12% bovine serum at 37°C and 5% CO_2. The cells were then cultured to the logarithmic phase for subsequent experiments.

2.1.3. Main Reagents. TPS of 99% active component (rhamnose, arabinose, xylose, glucose, galactose, galactoglucan, pectin, and protein) was purchased from Nanjing Tongying Biotechnology Co., Ltd. Fetal bovine serum, complete culture medium, and LipofectamineTM 2000 reagent were purchased from Invitrogen. Trizol and RNA extraction kits were purchased from Beijing Tianjian Biotechnology Co., Ltd. SYBR Premix Ex TaqTM II kit, PrimescripTM RT reagent kit, and miRNA PrimescripTM RT reagent kit were purchased from Takara. The primers were synthesized by Sangon Biotech (Shanghai, China). The H_2O_2 content kit was purchased from Beijing Solarbio Science & Technology Co., Ltd. The dual luciferase reporter gene kit was purchased from Beijing Baiao Laibo Co., Ltd. The protein extraction kit was purchased from NanJing KeyGen Biotech Co., Ltd. The Annexin V-PE/7-AAD apoptosis kit was purchased from Shanghai Yu Bo Biotechnology Co., Ltd.

2.2. Methods

2.2.1. MCAO Mouse Modeling and TPS Treatment. The cephalic flesh of the mice anesthetized with chloral hydrate was opened, the fascia of the skull surface was cleaned, and the probe of the laser Doppler flowmeter was fixed at a specific position on the skull. The supine skin was cut in the middle with tissues separated. The right common carotid artery, internal carotid artery, and external carotid artery were then exposed and ligated with 6-0 silk suture. The external carotid artery was separated using a microelectric coagulator, in which a small incision was made near bifurcation of the common carotid artery. A filament was inserted and tied to the incision in the external carotid artery with another silk suture. The ligated internal carotid artery was loosened, along which the filament was inserted slowly into the intracranial space to an approximate depth of 9 mm. After 60 min, the filament was pulled out, and the incision in the external carotid artery was ligated. The ligature of the common carotid artery was loosened, and the skin was sutured. The mice fully awake were then returned to their cages. The mice in sham operation group were performed the same as those in the operation group except the use of the filament. Mice in TPS treated groups were given intraperitoneal injection of TPS (0, 50, 100, 150, and 200 mg kg^{-1}) every 12 h for 72 h after reperfusion injury. The sham and model groups received an equal volume of saline per injection.

2.2.2. Detection of Cerebral Infarction Volume in Mice. The heads of mice, 72 h after cerebral ischemia and reperfusion, were removed from the body and frozen at −20°C for 30 min. The brain tissues serially sectioned at 2.0 mm were placed in 1% TTC phosphate buffer in a water bath at 37°C for 30 min. Afterwards, the sections were scanned, and the percentage of cerebral infarct volume to total brain volume was calculated by Image pro plus 5.1 software. The experiment was repeated 3 times.

TABLE 1: Primer sequence.

Gene	Forward primer	Reverse primer
miR-375	5′-CTTACTATCCGTTTGTTCGTTCG-3′	5′-TATGGTTGTTCTCGTCTCTGTGTC-3′
SRXN1	5′-TGCCAACCCTAGGAGGTAGA-3′	5′-CCCCAAGTTCCTGCCAGAAT-3′
Bcl-2	5′-ATCGCCCTGTGGATGACTGAG T-3′	5′-GCCAGGAGAAATCAAACAG AGGC-3′
Bax	5′-TCAGGATGCGTCCACCAAGAAG-3′	5′-TGTGTCCACGGCGGCAATCATC-3′
Caspase-3	5′-TGTGGCATTGAGACAGAC-3′	5′-CACTTGCCATACAAACTA-3′
U6	5′-CTCGCTTCGGCAGCACA-3′	5′-AACGCTTCACGAATTTGCGT-3′
GAPDH	5′-TCCTCTGACTTCAACAGCGACAC-3′	5′-CACCCTGTTGCTGTAGCCAAATTC-3′

2.2.3. Determination of Brain Water Content. The heads of mice, 72 h after cerebral ischemia and reperfusion, were removed from the body. The brains were obtained, and the wet weights were recorded. The brains were then dried to constant weight in an oven at 110–115°C to determine the dry weight. Brain water content was calculated with the following formula: water content = (wet weight − dry weight)/ wet weight × 100%. Three replicates were performed.

2.2.4. H_2O_2 Assay. The H_2O_2 content in mouse brain tissue was measured at 415 nm using the H_2O_2 content kit and a microplate reader.

2.2.5. Establishment of OGD/R Model. OGD/R treatment was utilized to simulate ischemia-reperfusion injury in vitro [20]. Briefly, the original DMEM medium was replaced with glucose-free DMEM for further AS incubation. The cells were incubated for 6 h in a hypoxic environment containing 5% CO_2, 1% O_2, and 94% N_2. The AS were subsequently transferred to normal DMEM medium and incubated for another 24 h.

2.2.6. Cell Proliferation Detection. AS harvested by scraping from the medium were placed in a serum-free solution, blown into individual cells, and cultured in suspension. The cells were then seeded onto 96-well plates at a density of 5000 per well with 20 μL per well, and TPS (0, 10, 20, 40, and 60 mg/L) were added, respectively. Afterwards, a solution of 10 μL MTT dissolved in PBS was added, and the cells were incubated at 37°C in 5% CO_2 for 4-6 h. The culture solution in the wells was then removed, and 150 μL of DMSO was added. After 10 min, the absorbance value was detected at 570 nm using a microplate reader. Three replicates were performed.

2.2.7. Apoptosis Detection. The cells in different groups were treated for 48 h and centrifuged at 600 × g for 5 min, the supernatant was discarded, and the cells were washed once with PBS. The cells in each group were seeded into 6-well plates at a density of 1×10^5 and cultured for 12 h. Apoptosis under different treatments was detected using Annexin V-PE/7-AAD Apoptosis Kit and flow cytometer (BD Biosciences, USA).

2.2.8. Real-Time Fluorescence Quantitative (qPCR). Total RNA of MA was extracted using TRIzol and an RNA extrac-tion kit. RNA quality and concentration were measured by NanoDrop and uniformly diluted to 500 ng μL^{-1}. RNA was then reverse transcribed into cDNA using PrimeScript RT and miRNA PrimeScriptTM RT kits, and primers were synthesized by Sangon Biotech (Shanghai, China). The SYBR Premix Ex TaqTM II kit was then used as a template for qPCR amplification. The LightCycler ® 96 Instrument (Roche, Switzerland) was used: initial denaturation at 95°C for 30 s, 40 cycles of denaturation at 95°C for 5 s followed by annealing/extension at 60°C for 30 s. GAPDH and U6 were used as internal references for mRNA and miRNA, and relative mRNA expression was calculated using $2^{-\Delta\Delta Ct}$ method. The sequences of the primers used for the fluorescent quantitative PCR are shown in Table 1. Three replicates were performed.

2.2.9. Western Blotting. Proteins were isolated from cells using RIPA. The protein mixture (with loading buffer) at the same concentration was boiled for 10 min at 95°C. Then, 20 μL of the mixture (containing 30–50 μg of sample) was added to a plate of 10% polyacrylamide gel and subjected to electrophoresis to separate proteins. The proteins were transferred from the gel to a PVDF membrane, blocked, and then incubated overnight at 4°C with primary antibodies. Samples were washed with TBST and incubated with secondary antibodies for 1 h at room temperature. β-Actin was used as an internal reference, and grayscale was determined with Image J. Three replicates were performed.

2.2.10. Cell Transfection. Cells in the logarithmic growth phase were taken and prepared for cell suspensions. The 1×10^5 cells were seeded in 6-well plates and incubated at 37°C and 5% CO_2 for 24 h. Lipofectamine 2000: DNA complexes were mixed gently and then allowed to stand. After incubation at room temperature for 20 min, the supernatant of cell culture medium was added, mixed, and cultured for another 24 h. Transfection efficiency of miRNA or mRNA was examined using RT-PCR and Western blotting. Three replicates were performed.

2.2.11. Dual-Luciferase Reporter Assay. Cells in logarithmic growth phase were cultured in 96-well plates, and cells with 80% confluence were obtained for transfection followed by another 48 h of culture. The 100 μL of lysate was added per well, and the solution was centrifuged at 12000 rpm for
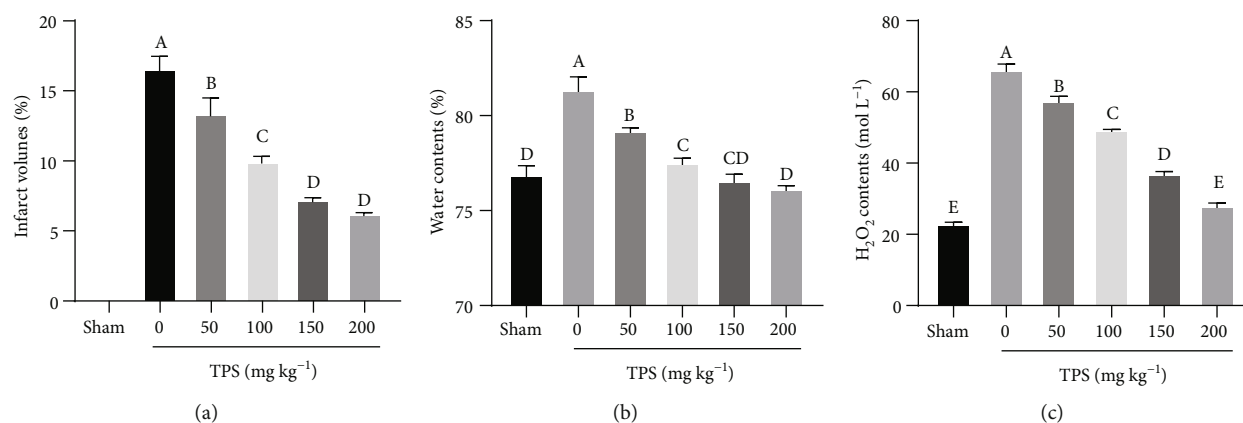
Figure 1: The effect of TPS on cerebral infarct volume, brain water content, and H2O2 content after cerebral ischemia-reperfusion injury. (a) Infarct volumes under different TPS concentration treatments. (b) Brain water contents under different TPS concentration treatments. (c) H2O2 contents under different TPS concentration treatments.

5 min. The supernatant ($50 \mu L$) was transferred into a 96-well plate, and then $40 \mu L$ of firefly luciferase assay substrate was added to each well and mixed by gentle shaking for 10 s to detect the fluorescence intensity. An additional $40 \mu L$ of Renilla luciferase assay substrate was added to the 96-well plate and mixed gently for 10 s to measure luciferase activity using a Glomax luminometer (Promega, USA). Three replicates were performed.

2.3. Statistical Analysis. Data analyses and drawing of statistical charts were performed using a GraphPad Prism 8 software. Differences in data between groups were statistically analyzed using Student's t-test and one-way ANOVA. $P < 0.05$ was considered statistically significant, $P < 0.01$ highly significant, and $P < 0.001$ extremely highly significant.

3. Results

3.1. TPS Ameliorated Cerebral Ischemia-Reperfusion Injury. The cerebral infarct area (Figure 1(a)) and brain water content (Figure 1(b)) in cerebral ischemia-reperfusion mice showed a gradual decrease with the increase of TPS concentration in the treatment groups as compared with the group without TPS administration. The H_2O_2 content in the brain tissues was measured, and it was found that the content gradually decreased as the concentration of TPS increased in the brain tissues with cerebral ischemia-reperfusion injury (Figure 1(c)).

3.2. TPS Reduced OGD/R-AS Apoptosis. The effect of TPS on AS proliferation under OGD/R treatment was examined using MTT assay, and the results revealed that AS cell viability was gradually enhanced with increasing TPS concentration, with the highest cell viability under $40 \, \text{mg} \, \text{L}^{-1}$ treatment (Figure 2(a)). Therefore, 0 and $40 \, \text{mg} \, \text{L}^{-1}$ of TPS were used in subsequent experiments. Flow cytometry to detect AS apoptosis revealed that 48 h after the TPS ($40 \, \text{mg} \, \text{L}^{-1}$) treatment, the level of AS apoptosis significantly declined compared with that of the control group (Figure 2(b)). Meanwhile, the results of qPCR and Western

blotting assays indicated that both mRNA and protein expression levels of the apoptosis-inhibiting Bcl-2 were increased, while mRNA and protein expression levels of the apoptosis-promoting Bax and caspase-3 were inhibited (Figures 2(c) and 2(d)).

3.3. TPS Reduced OGD/R-AS Apoptosis by Inhibiting the Expression of miR-375. The expression of miR-375 in AS was examined under different concentrations of TPS treatment, and the results revealed that miR-375 expression showed a decreasing trend with increasing TPS concentration (Figure 3(a)). To further examine the role of miR-375 in OGD/R-induced AS apoptosis, miR-375 mimics vector was constructed to transfect OGD/R-treated AS. The expression of miR-375 in AS was examined using QPCR, and we found that as compared with the control group, miR-375 mimics transfection increased miR-375 expression in AS (Figure 3(b)). Cell proliferation was detected by MTT assay, and the results revealed that overexpression of miR-375 inhibited cell proliferation, while the coeffect of miR-375 overexpression and TPS treatment partially suppressed cell proliferation (Figure 3(c)). Contrary to AS proliferation, the overexpression of miR-375 increased the apoptotic rate, while miR-375 overexpression and TPS treatment could partially alleviate apoptosis (Figure 3(d)). The results of qPCR and Western blotting showed that the mRNA and protein levels of apoptosis-related Bcl-2, Bax, and caspase-3 were consistent with the cell apoptosis (Figures 3(e) and 3(f)).

3.4. MiR-375 Targeted SRXN1. The miR-375 and SRXN1 target binding sites were first predicted by bioinformatics tools (starBase) (Figure 4(a)). In addition, the interaction between miR-375 and SRXN1 was validated using a dual luciferase reporter assay, and Figure 4(b) showed that the luciferase activity was significantly lower in cells transfected with miR-375 mimics+SRXN1-WT than in miR-375 NC+SRXN1-WT transfected cells. Transfection of SRXN1-MUT had no significant effect on the luciferase activity. The results of qPCR and Western blotting showed increased mRNA and proteins expression levels of SRXN1
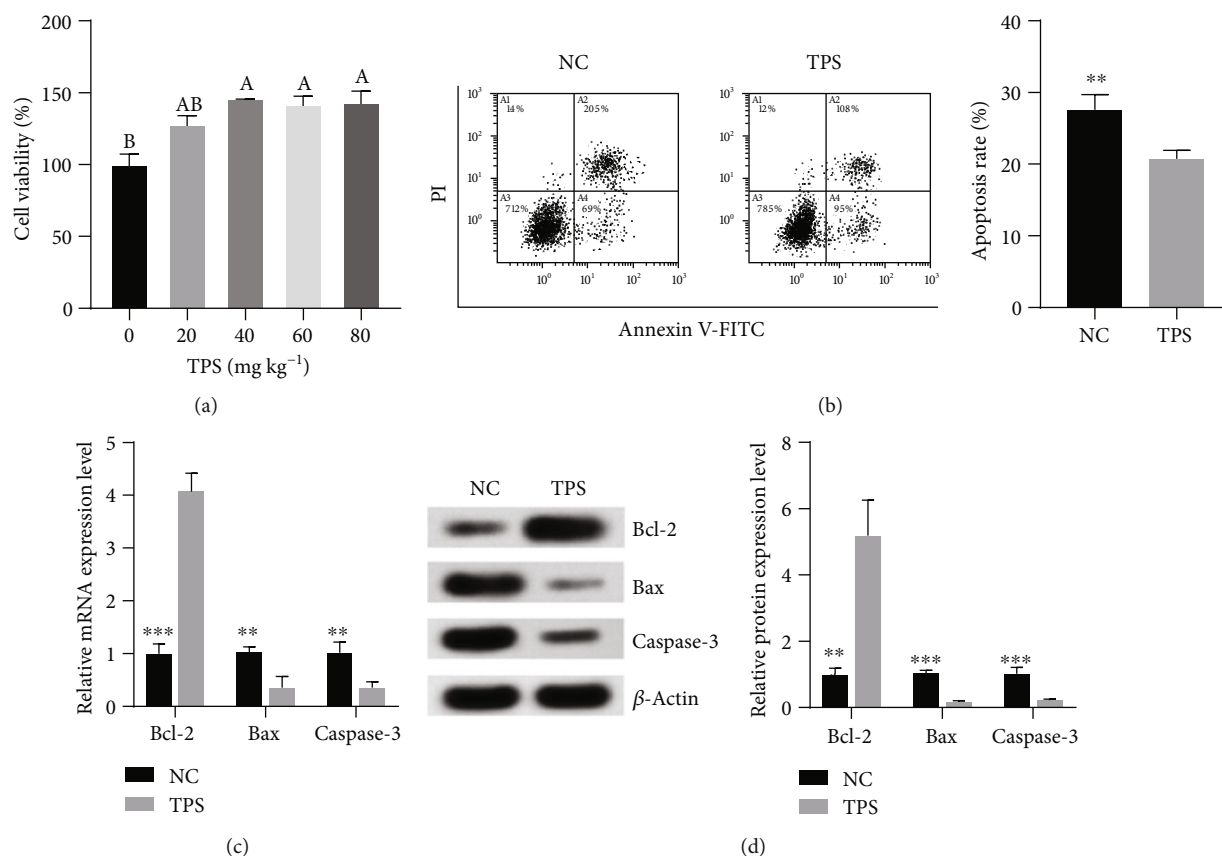
(a)

(b)

(c)

(d)

FIGURE 2: Effects of TPS on OGD/R-AS cell viability and apoptosis. (a) Cell viability of AS under different TPS concentration treatments. (b) Cell apoptosis rate of AS. (c) Relative mRNA expression level of apoptosis-related proteins. (d) Relative protein expression level of apoptosis-related proteins. Note: each treatment in the figure has different lowercase letters, which means that the difference between the different treatments is significant ($P < 0.05$). $^{**}P < 0.01$, $^{***}P < 0.001$ compared with NC group. NC: negative control.

in cells transfected with miR-375 inhibitor (Figures 4(c) and 4(d)).

3.5. miR-375/SRXN1 Axis Mediated TPS to Reduce OGD/R-Induced AS Injury. First, the transfection efficiency as well as the effect of overexpression of miR-375 on SRXN1 expression in AS were examined using qPCR and Western blotting. It was found that SRXN1 overexpression increased mRNA levels and protein levels of SRXN1in OGD/R-treated AS, whereas miR-375 overexpression suppressed the mRNA and protein levels of SRXN1. Furthermore, overexpression of SRXN1 and miR-375 could restore the suppressed SRXN1 expression (Figures 5(a) and 5(b)). Subsequently, the effect of miR-375/SRXN1 on cell viability and apoptosis was examined. The overexpression of SRXN1 and TPS treatment significantly increased cell viability, whereas overexpression of SRXN1 and miR-375 showed no difference in cell viability (Figure 5(c)). Compared with TPS treatment, the coeffect of overexpression of SRXN1 and TPS treatment resulted in a lower rate of apoptosis, but there was no difference in apoptosis when SRXN1 and miR-375 were cooverexpressed (Figure 5(d)). The qPCR and Western blotting results showed that SRXN1 overexpression along with TPS treatment increased the expression of Bcl-2, the inhibitor of apo-

ptosis protein, and decreased the expression of Bax and caspase-3, the proapoptotic proteins, while simultaneous overexpression of SRXN1 and miR-375 restored the expression levels of Bcl-2, Bax, and caspase-3 to the levels when only TPS was added (Figures 5(e) and 5(f)).

4. Discussion

As food-derived polysaccharides, TPS are widely found in various teas such as black tea, green tea, and dark green tea [21] and has been proven to have many biological functions. Moreover, we confirmed in this study that TPS alleviates OGD/R-induced AS apoptosis in vitro, and verified its possible molecular mechanism.

Cerebral ischemia and reperfusion triggers a series of inflammatory reactions, oxidative stress, and apoptosis, which leads to the breakdown of the blood-brain barrier, resulting in brain edema and exacerbation of nerve injury. There is evidence that AS-derived factors play a critical role in the destruction and recovery of the blood-brain barrier following brain injury [22]. AS have been used as a major therapeutic target in brain diseases, and studies have shown that better control of AS helps reduce brain injury in various experimental animal models [4].
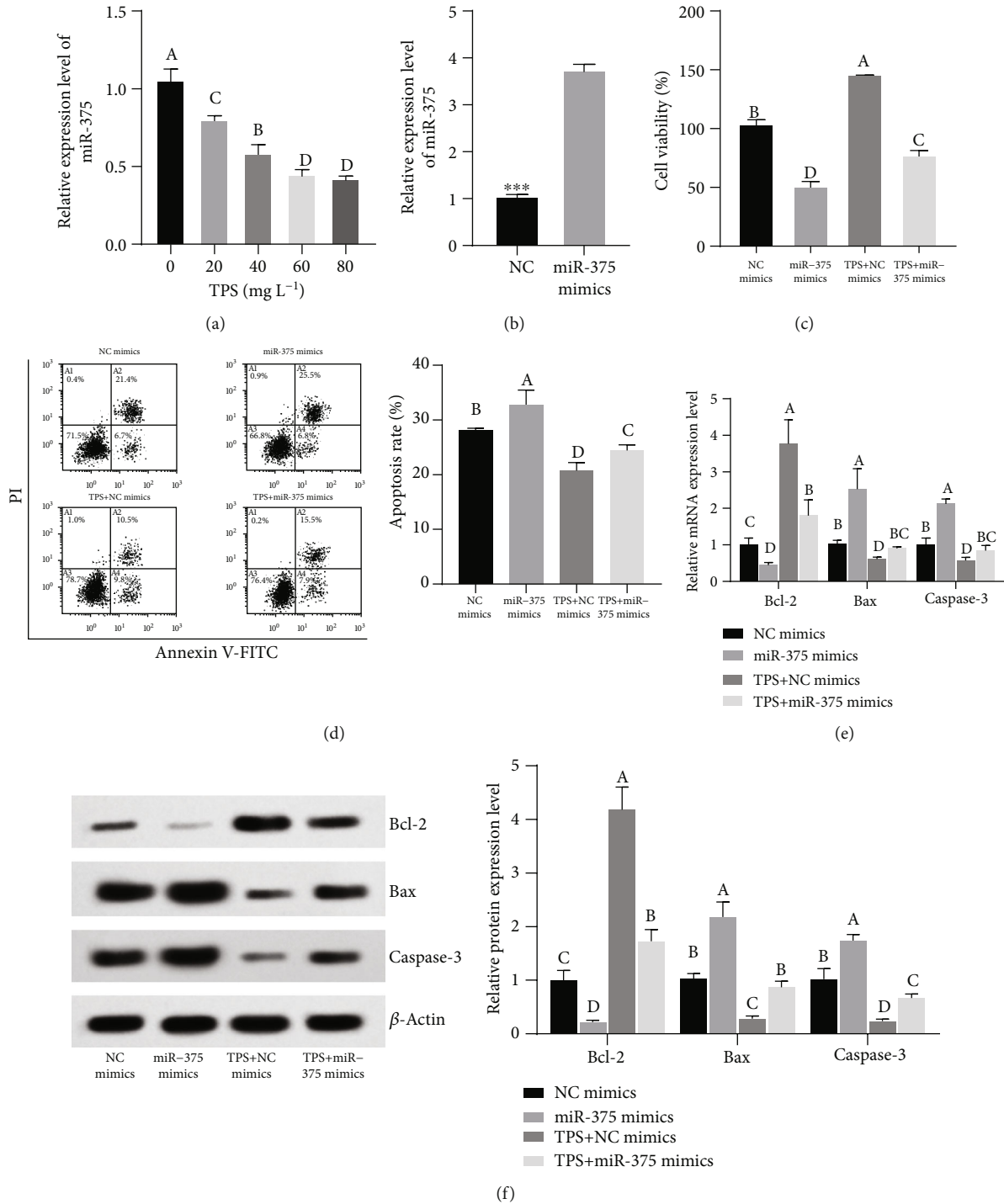
(a)

(b)

(c)

(d)

(e)

(f)

Figure 3: TPS increased cell viability and reduced apoptosis of OGD/R-AS through inhibiting the expression of miR-375. (a) Relative expression of miR-375 under different TPS concentration treatments. (b) Transfection efficiency of miR-375 mimics. (c) Cell viability of AS. (d) Cell apoptosis rate of AS. (e) Relative mRNA expression level of apoptosis-related proteins. (f) Relative protein expression level of apoptosis-related proteins. Note: each treatment in the figure has different lowercase letters, which means that the difference between the different treatments is significant ($P < 0.05$), $P < 0.001$ compared with NC group. NC: negative control.

Therefore, AS are essential for protecting the integrity of the blood-brain barrier. Our study also demonstrated that OGD/R-AS treated by TPS show significant increase in its activity.

Accumulating evidence suggests that miRNAs act as key modulators of cellular activation and inflammatory responses [23]. Guo et al. [24] reported that miR-375 induced ROS production and apoptosis in cells by
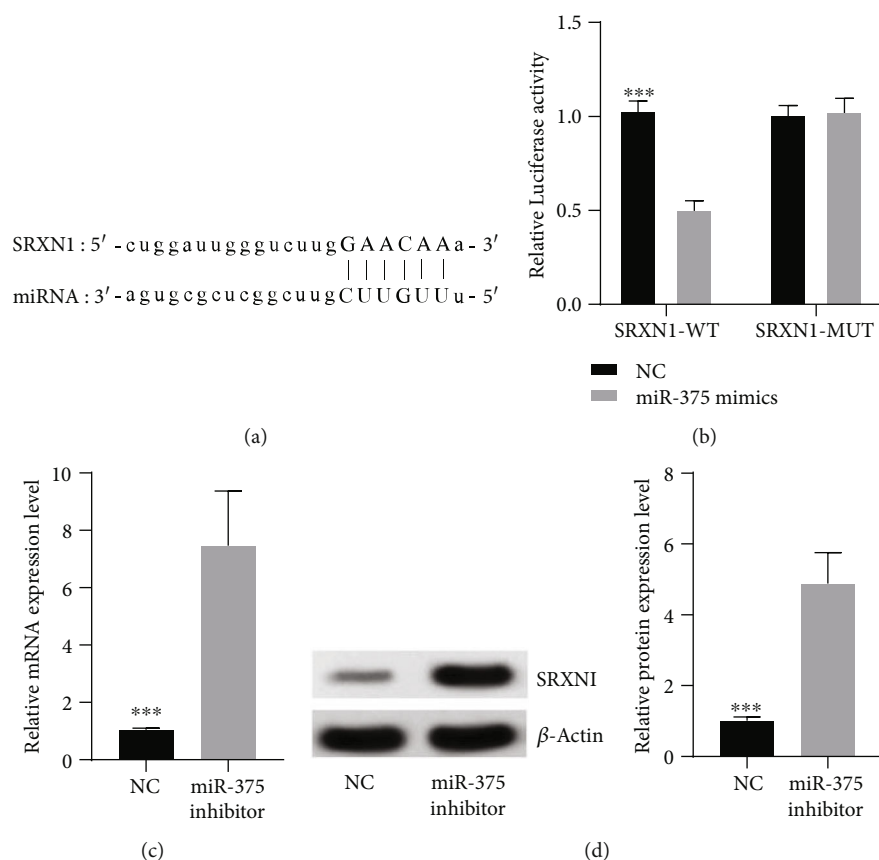
SRXN1 : 5′ - c u g g a u u g g g u c u u g G A A C A A a - 3′
| | | | | |
miRNA : 3′ - a g u g c g c u c g g c u u g C U U G U U u - 5′

(a)

(b)

(c)

(d)

FIGURE 4: miR-375 directly targeted SRXN1and regulated the expression of SRXN1. (a) The binding site of miR-375 and SRXN1. (b) Dual-luciferase relative activity. (c) Relative mRNA expression level of SRXN1. (d) Relative protein expression level of SRXN1. Note: ***$P < 0.001$ compared with NC group. NC: negative control.

targeting HIGD1A. MiR-375 (miR-375) plays an important role in the development and progression of cervical cancer, inhibits cell proliferation, and promotes apoptosis by targeting IGF-1R [25]. In addition, upregulation of miR-375 can also inhibit HCC cell proliferation and promote apoptosis by targeting ErbB2 [26]. We found in this study that miR-375 could modulate AS activity by targeting SRXN1. The antioxidant role of SRXN1 has been widely reported, and SRXN1 protects brain tissue from damage by regulating glutathionylation/deglutathionylation in Parkinson's disease [27]. Moreover, induction of SRXN1 expression contributes to neuronal protection in response to oxygen-glucose deprivation after brief ischemic episodes in vitro and in vivo [28]. However, there are few reports on the role of SRXN1 in cerebral ischemia-reperfusion injury and apoptosis-induced injury. In our study, TPS was found to indirectly regulate SRXN1 expression through miR-375, suggesting a protective role of SRXN1 in AS apoptosis that was caused by oxidative stress. It also provided a basis for studying the molecular mechanism of SRXN1 in cerebral ischemia-reperfusion injury.

However, this study also has some limitations. The blood-brain barrier in the body can effectively filter substances entering and exiting the brain to protect the brain from external damage [29]. TPS, as a macromolecule, like other drugs in the body, may be restricted by the blood-brain barrier from entry into the brain. The results of this study showed that brain injury was significantly reduced after TPS treatment in mice, which may be due to the fact that some small pivotal components of TPS can permeate through the membrane of the intestinal epithelial barrier and blood-brain barrier. It has been reported that blood brain barrier permeability via caveolae-dependent endocytosis transports small molecules such as lipids into the brain [30]. However, it is necessary to further determine the small molecules that play a role in TPS, in order to promote the further study on protective effect of TPS on cerebral ischemia-reperfusion injury. In addition, given that the small molecules may regulate miRNAs by activating a series of complex intracellular signaling pathways to after entering the cell, studying the mechanism of miRNA regulation by polysaccharides in vivo also helps to explain how polysaccharides exert anti-inflammatory and antioxidant effect. Therefore, there is an urgent need to find a way to get the active molecules through the blood-brain barrier into the brain.

In summary, our study demonstrated that TPS alleviates AS injury induced by cerebral ischemia reperfusion both in vivo and in vitro, which is based on the inhibition of AS
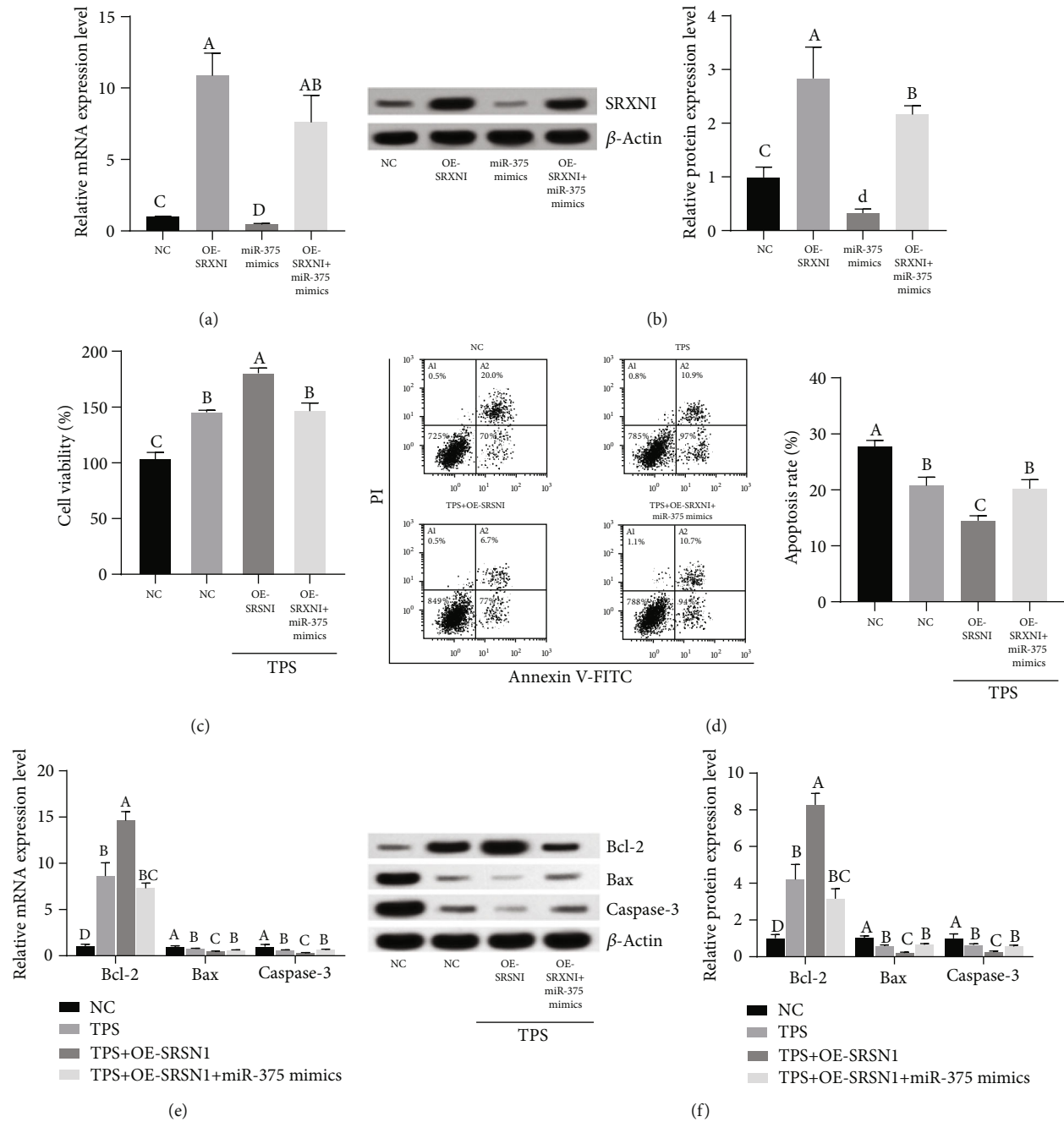
(a)

(b)

(c)

(d)

(e)

(f)

FIGURE 5: TPS alleviated damage of OGD/R AS via regulating miR-375/SRXN1 axis. (a) Transfection efficiency of OE-SRXN1 and/or miR-375 mimics and the effect of miR-375 on SRXN1 mRNA expression level. (b) Transfection efficiency of OE-SRXN1 and/or miR-375 mimics and the effect of miR-375 on SRXN1 protein expression level. (c) Cell viability of AS. (d) Cell apoptosis rate of AS. (e) Relative mRNA expression level of apoptosis-related protein. (f) Relative protein expression level of apoptosis-related protein. Note: each treatment in the figure has different lowercase letters, which means that the difference between the different treatments is significant ($P < 0.05$). NC: negative control.

apoptosis by regulating miR-375/SRXN1 axis. This provides a theoretical basis for the TPS clinical treatment in ischemia-reperfusion injury.

Data Availability

The data and materials used to support the findings of this study are included within the published article.

Conflicts of Interest

The authors declare that they have no conflicts of interest.

Acknowledgments

References

[1] T. Gattringer, A. Posekany, K. Niederkorn et al., "Predicting early mortality of acute ischemic stroke," *Stroke*, vol. 50, no. 2, pp. 349–356, 2019.

[2] V. Janardhan and A. I. Qureshi, "Mechanisms of ischemic brain injury," *Current Cardiology Reports*, vol. 6, no. 2, pp. 117–123, 2004.

[3] Y. P. Zhang, Y. Zhang, Z. B. Xiao et al., "CFTR prevents neuronal apoptosis following cerebral ischemia reperfusion via regulating mitochondrial oxidative stress," *Journal of Molecular Medicine*, vol. 96, no. 7, pp. 611–620, 2018.

[4] S. Michinaga and Y. Koyama, "Dual roles of astrocyte-derived factors in regulation of blood-brain barrier function after brain damage," *International Journal of Molecular Sciences*, vol. 20, no. 3, p. 571, 2019.

[5] A. Kinsner, V. Pilotto, S. Deininger et al., "Inflammatory neurodegeneration induced by lipoteichoic acid from Staphylococcus aureus is mediated by glia activation, nitrosative and oxidative stress, and caspase activation," *Journal of Neurochemistry*, vol. 95, no. 4, pp. 1132–1143, 2005.

[6] S. G. Rhee, W. Jeong, T. S. Chang, and H. A. Woo, "Sulfiredoxin, the cysteine sulfinic acid reductase specific to 2-Cys peroxiredoxin: its discovery, mechanism of action, and biological significance," *Kidney International*, vol. 72, pp. S3–S8, 2007.

[7] J. Wu, Y. Chen, S. Yu et al., "Neuroprotective effects of sulfiredoxin-1 during cerebral ischemia/reperfusion oxidative stress injury in rats," *Brain Research Bulletin*, vol. 132, pp. 99–108, 2017.

[8] A. P. Vivancos, E. A. Castillo, B. Biteau et al., "A cysteine-sulfinic acid in peroxiredoxin regulates H2O2-sensing by the antioxidant Pap 1 pathway," *Proceedings of the National Academy of Sciences*, vol. 102, no. 25, pp. 8875–8880, 2005.

[9] F. X. Soriano, F. Léveillé, S. Papadia et al., "Induction of sulfiredoxin expression and reduction of peroxiredoxin hyperoxidation by the neuroprotective Nrf 2 activator 3H-1, 2-dithiole-3-thione," *Journal of Neurochemistry*, vol. 107, no. 2, pp. 533–543, 2008.

[10] Y. Zhou, Y. Zhou, S. Yu, J. Wu, Y. Chen, and Y. Zhao, "Sulfiredoxin-1 exerts anti-apoptotic and neuroprotective effects against oxidative stress-induced injury in rat cortical astrocytes following exposure to oxygen-glucose deprivation and hydrogen peroxide," *International Journal of Molecular Medicine*, vol. 36, no. 1, pp. 43–52, 2015.

[11] L. Guo, Q. Liang, and X. Du, "Effects of molecular characteristics of on konjac glucomannan glass transitions of potato amylose, amylopection and their mixtures," *Journal of the Science of Food and Agriculture*, vol. 91, no. 4, pp. 758–766, 2011.

[12] W.-Y. Huang, S. T. Davidge, and J. Wu, "Bioactive natural constituents from food sources-potential use in hypertension prevention and treatment," *Critical Reviews in Food Science and Nutrition*, vol. 53, no. 6, pp. 615–630, 2013.

[13] D. Ren, Y. Hu, Y. Luo, and X. Yang, "Selenium-containing polysaccharides from Ziyang green tea ameliorate high-fructose diet induced insulin resistance and hepatic oxidative stress in mice," *Food function*, vol. 6, no. 10, pp. 3342–3350, 2015.

[14] P. Xu, J. Wu, Y. Zhang, H. Chen, and Y. Wang, "Physicochemical characterization of puerh tea polysaccharides and their antioxidant and α-glycosidase inhibition," *Journal of Functional Foods*, vol. 6, pp. 545–554, 2014.

[15] Y. Wang, S. Shao, P. Xu et al., "Fermentation process enhanced production and bioactivities of oolong tea polysaccharides," *Food Research International*, vol. 46, no. 1, pp. 158–166, 2012.

[16] M. Pu, J. Chen, Z. Tao et al., "Regulatory network of miRNA on its target: coordination between transcriptional and post-transcriptional regulation of gene expression," *Cellular and Molecular Life Sciences*, vol. 76, no. 3, pp. 441–451, 2019.

[17] R. Herzog, A. Zendedel, L. Lammerding, C. Beyer, and A. Slowik, "Impact of 17beta-estradiol and progesterone on inflammatory and apoptotic microRNA expression after ischemia in a rat model," *The Journal of Steroid Biochemistry and Molecular Biology*, vol. 167, pp. 126–134, 2017.

[18] Y. Liu and Y. Zhang, "Lycium barbarum polysaccharides alleviate hydrogen peroxide-induced injury by up-regulation of miR-4295 in human trabecular meshwork cells," *Experimental and Molecular Pathology*, vol. 106, pp. 109–115, 2019.

[19] Y. Ruan, H. Li, L. Pu, T. Shen, and Z. Jin, "Tremella fuciformis polysaccharides attenuate oxidative stress and inflammation in macrophages through miR-155," *Analytical Cellular Pathology*, vol. 2018, Article ID 5762371, 10 pages, 2018.

[20] Y. Cao, H. Liu, J. Zhang, and Y. Dong, "Circular RNA cZNF292 silence alleviates OGD/R-induced injury through up-regulation of miR-22 in rat neural stem cells (NSCs)," *Artificial Cells, Nanomedicine, and Biotechnology*, vol. 48, no. 1, pp. 594–601, 2020.

[21] H. Chen, Z. Qu, L. Fu, P. Dong, and X. Zhang, "Physicochemical properties and antioxidant capacity of 3 polysaccharides from green tea, oolong tea, and black tea," *Journal of Food Science*, vol. 74, no. 6, pp. C469–C474, 2009.

[22] R. Eilam, M. Segal, R. Malach, M. Sela, R. Arnon, and R. Aharoni, "Astrocyte disruption of neurovascular communication is linked to cortical damage in an animal model of multiple sclerosis," *Glia*, vol. 66, no. 5, pp. 1098–1117, 2018.

[23] M. Mann, A. Mehta, J. L. Zhao et al., "An NF-κB-microRNA regulatory network tunes macrophage inflammatory responses," *Nature Communications*, vol. 8, no. 1, p. 851, 2017.

[24] J. Guo, C. Yang, S. Zhang et al., "MiR-375 induces ROS and apoptosis in ST cells by targeting the HIGD1A gene," *Gene*, vol. 685, pp. 136–142, 2019.

[25] X. Yu, W. Zhao, X. Yang, Z. Wang, and M. Hao, "miR-375 affects the proliferation, invasion, and apoptosis of HPV16-positive human cervical cancer cells by targeting IGF-1R," *International Journal of Gynecological Cancer*, vol. 26, no. 5, pp. 851–858, 2016.

[26] L. Li, L. Jia, and Y. Ding, "Upregulation of miR-375 inhibits human liver cancer cell growth by modulating cell proliferation and apoptosis via targeting ErbB2," *Oncology Letters*, vol. 16, no. 3, pp. 3319–3326, 2018.

[27] V. J. Findlay, H. Tapiero, and D. M. Townsend, "Sulfiredoxin: a potential therapeutic agent?," *Biomedicine & Pharmacotherapy*, vol. 59, no. 7, pp. 374–379, 2005.

[28] K. F. Bell, B. al-Mubarak, J. H. Fowler et al., "Mild oxidative stress activates Nrf2 in astrocytes, which contributes to neuroprotective ischemic preconditioning," *Proceedings of the National Academy of Sciences*, vol. 108, no. 1, pp. E1–E2, 2011.

[29] S. Liebner, R. M. Dijkhuizen, Y. Reiss, K. H. Plate, D. Agalliu, and G. Constantin, "Functional morphology of the blood-brain barrier in health and disease," *Acta Neuropathologica*, vol. 135, no. 3, pp. 311–336, 2018.

[30] B. J. Andreone, B. W. Chow, A. Tata et al., "Blood-brain barrier permeability is regulated by lipid transport-dependent suppression of caveolae-mediated transcytosis," *Neuron*, vol. 94, no. 3, pp. 581–594.e5, 2017.